*Desalination and Water Treatment*
www.deswater.com

doi: 10.1080/19443994.2013.846239

53 (2015) 818–825
January

Taylor & Francis
Taylor & Francis Group

# Removal of basic dyes (malachite green) from aqueous medium by adsorption onto amino functionalized graphenes in batch mode

Xiaoyao Guo[a], Qin Wei[b], Bin Du[a,*], Yakun Zhang[a], Xiaodong Xin[a], Liangguo Yan[a], Haiqin Yu[b]

[a]*School of Resources and Environment, University of Jinan, Jinan 250022, China*
*Tel. +86 531 82767872; Fax: +86 531 82767370; email: dubin61@gmail.com*
[b]*School of Chemistry and Chemical Engineering, University of Jinan, Jinan 250022, China*

Received 3 July 2013; Accepted 29 August 2013

ABSTRACT

In this paper, graphene oxides and amino functionalized graphenes ($NH_2$-G) were prepared and employed as adsorbent for the removal of a basic dye, malachite green (MG). The effect of several parameters (pH, dye concentration, adsorption time, and temperature) of the adsorption process was investigated for $NH_2$-G. Four different adsorption isotherms were used to analyze the equilibrium of the adsorption system. The adsorption mechanism was investigated by adsorption thermodynamics and adsorption kinetics. The results indicated that $NH_2$-G showed a high efficiency for the removal of the basic dye MG with the maximum adsorption capacity of 91.48 mg $g^{-1}$. According to the obtained thermodynamic data, the adsorption of MG onto $NH_2$-G was an endothermic process with a large adsorption enthalpy. The kinetic study showed that the whole adsorption process fit the pseudo-second-order kinetics model well.

*Keywords:* Malachite green; Amino-functionalized graphenes; Adsorption isotherm; Adsorption kinetics; Thermodynamics

## 1. Introduction

Dyes are extensively used as coloring agents in industries, including textile, leather, paper, and food. About 10–15% of these dyes are released in effluents during dyeing process [1]. Waste effluents containing these coloring agents may cause severe environmental pollution and serious threat to human health due to their toxic and carcinogenic properties [2]. Dyes are also known to impart highly obvious color to water which is very undesirable to the water consumer and can deleteriously affect the photosynthetic aquatic life due to the reduction of light penetration [3,4]. Therefore, the removal of dyes from industrial effluents should be given considerable attention.

However, the dyes are difficult to be removed from aqueous solutions, especially those containing azo groups, since they are highly stable and resistant to heat, light, and oxidizing agents [5]. To date, numerous of treatments, such as biological treatment, coagulation and flocculation, ozone treatment, chemical oxidation, membrane filtration, ion exchange, photocatalytic degradation and adsorption, have been developed [6–14]. Adsorption has been investigated as an efficient and economical technique to remove dyes. Hence, there is

*Corresponding author.

an avid intensive study for the adsorption technique to the dye-contained wastewater treatment.

Recently, graphite oxides (GO) and functionalized graphenes have aroused a strong interest due to their extraordinary properties, such as the chemical stability, large surface area, and hydrophility [15,16]. They have enormous applications in sensors, nanoelectronics, batteries, hydrogen storage and nanocomposites [17,18]. The large theoretical specific surface area of graphene ensures the excellent adsorption capacity, especially for those planar compounds [19]. Up to now, many functionalized adsorbents based on graphene have been extensively used to remove contaminants from aqueous solutions. For example, it was found that sulfonated graphene is one of the most effective adsorbents to remove naphthalene and 1-naphthol [20]. GO *in situ* reduction with sodium hydrosulfite could effectively remove acridine orange [21]. Graphene nanosheets have high adsorption affinity for heavy metals, where the amount of active surface sites on graphene is an important factor influencing the adsorption of heavy metal ions [22]. However, few investigations have been reported about the application of graphene derivatives as adsorbent to remove dyes. In this study, amino-functionalized graphenes ($NH_2$-G) was synthesized and characterized by TEM, FTIR, XRD, and BET analyses. In order to further investigate the interaction between the functionalized graphenes and the organic dyestuff molecules, the kinetic and thermodynamic studies were carried out on malachite green (MG) (Fig. 1), a basic dye, adsorbed by $NH_2$-G. The $NH_2$-G has high dispersion properties in aqueous solution, which ensures its high interaction with dye molecules. The adsorption measurements showed that $NH_2$-G is a promising material to adsorb dyes due to their large quantities of amino which present on the surface of the resulting $NH_2$-G [23].

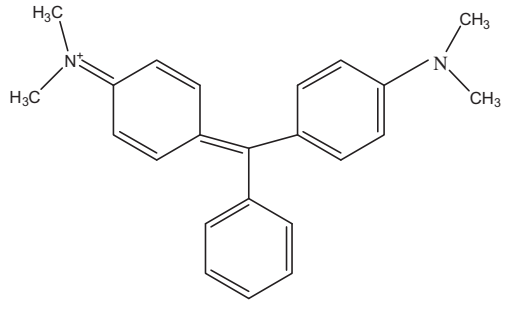


Fig. 1. Structure of malachite green.

## 2. Experimental

### 2.1. Reagents and solutions

All chemicals used in the experiment were obtained from Sinopharm Chemical Reagent Beijing Co., Ltd, China, which are analytical reagent grade or better quality. The solutions were prepared with ultrapure water (EASY-pure LF, Barnstead International, Dubuque, Iowa USA). About 40 mg $L^{-1}$ stock solutions of MG were prepared by dissolving MG in ultrapure water. These solutions were kept in the dark.

### 2.2. Preparation of adsorbent

#### 2.2.1. Preparation of GO

The GO were synthesized from graphite powder according to the improved method reported by Daniela C. Marcano [24]. A mixture of concentrated $H_2SO_4/H_3PO_4$ (36/4 mL) was added into a 3-neck flask with 0.3 g graphite powder and 1.8 g $KMnO_4$. The mixtures were stirred vigorously at 50°C for 12 h and allowed to cool down to room temperature with 0.3 mL 30% $H_2O_2$. The product was centrifuged (8,000 rpm for 30 min), and the supernatant was decanted away. The remaining solid material was then washed two times with HCl (0.2 mol $L^{-1}$), ethanol and ether. Afterwards, the obtained solid was vacuum-dried at 35°C.

#### 2.2.2. Preparation of $NH_2$-G

The prepared GO (100 mg) was addition to 40 mL of ethylene glycol under ultrasonication, followed by the addition of 1 ml of ammonia water. Then, the dark brown solution was transferred into Teflon-lined autoclave. They were heated and maintained at 180°C for 10 h. After the reaction, the precipitate was washed repeatedly with distilled water and vacuum-dried at 50°C [16].

### 2.3. Characterization methods

The morphology of $NH_2$-G was investigated by TEM images that were obtained from a JEM-2100 microscope (JEOL, Japan). BET analysis was performed on Micromeritics ASAP 2020 surface area and porosity analyzer (Quantachrome, United States). Pore distributions and pore volume were calculated using the adsorption branch of the $N_2$ isotherms based on the BJH model. FTIR spectra were recorded in the spectral range of 4,000–400 $cm^{-1}$ on Perkin–Elmer spectrum One FTIR spectrometer (Perkin–Elmer, United States). X-ray diffractometer (XRD) patterns of

the prepared samples were acquired with Rigaku D/MAX 2200 XRD (Tokyo, Japan).

### 2.4. Procedure of dye adsorption

In a typical batch-adsorption experiment procedure, 10 mg of adsorbent agitate with 25 mL of solution containing known concentration of MG in an air-tight conical flask for 150 min, the mixture was adjusted to pH as neutrality by HCl and NaOH.

To investigate the effect of pH, 25 mL of 40 mg $L^{-1}$ MG with pH ranging from 3.0 to 11.0 was mixed with 10 mg of $NH_2$-G agitate for 150 min at 298 K. For the adsorption kinetic experiments, the $NH_2$-G was also investigated with contacting time ranging from 5 to 210 min at pH 8.0. In order to obtain the adsorption isotherms of the dye, solutions with different initial concentration (10–120 mg $L^{-1}$) were treated with the same procedure as above at 298 K. The bath experiment for adsorption thermodynamics of MG was also carried out at varying temperatures (298, 308, and 318 K) with different initial concentrations.

The solution and phase were separated by centrifugation at 9,500 rpm for 30 min. Thereafter, the residual dye in the supernatant was measured with UV-spectrophotometer (Lambda35 UV/vis spectrometer, Perkin–Elmer), at the maximum absorbance wavelength of MG ($\lambda_{max}$ = 618 nm).

The removal efficiency and the amount of dye adsorbed $q_t$ (mg $g^{-1}$) were given according to the formula:

$$\text{Removal efficiency } (\%) = \frac{c_0 - c_t}{c_0} \times 100\% \quad (1)$$

$$q_t = (c_0 - c_t) \times V/m \quad (2)$$

where $c_t$ (mg $L^{-1}$) is the concentration of adsorbate at time $t$ (min), $V$ (L) is the volume of adsorbate, $m$ (g) is the mass of adsorbents. $q_t$ (mg $g^{-1}$) is the adsorbed amount at time $t$ (min).

## 3. Results and discussion

### 3.1. Characteristics of adsorbent

The morphology of $NH_2$-G was investigated by TEM image, and the fold structure can be seen clearly according to Fig. 2(a).

The XRD patterns of $NH_2$-G and GO were acquired with Cu$K\alpha$ radiation (40 kV, 300 mA) of wavelength 0.154 nm, to confirm the structure of the materials. It can be seen the typical diffraction peak of GO at 10˚, while there is no typical diffraction peak of $NH_2$-G which given further support that GO has translated into $NH_2$-G (Fig. 2(b) and (c)).

Fig. 2(d) exhibits the FTIR spectra of $NH_2$-G and GO. In the FTIR spectrum of GO, we observe a strong and broad absorption at 3,433 $cm^{-1}$ due to O–H stretching vibration. The major absorption bands characteristic of the C=O stretching of COOH groups lay in 1,724 $cm^{-1}$. The absorption due to the O–H bending vibration and epoxide groups are observed around 1,637 $cm^{-1}$. The appearance of a band in the IR spectrum of $NH_2$-G at 3,425 $cm^{-1}$ may be attributed to the $NH_2$, which confirms the presence of amide functional group [16,25].

The BET analysis of $NH_2$-G was shown in Fig. 2(e). According to the BET analysis, the isotherm is of type III and displays the D hysteresis loop and the surface area of $NH_2$-G is 359.8 $m^2 g^{-1}$.

### 3.2. Effect of pH on the removal of MG

The effect of pH on the removal of MG is very important in the following three points. First, the type and magnitude of charge on the dye species predominating in solution will determine whether the removal will take place or not. Secondly, the magnitude of the charge of the dye will determine the molar ratio adsorbent/dye suitable for the maximum removal of dye. Thirdly, the nature of the dye predominant in the solution determines the state of the collector/dye, and therefore, determines the mechanism of the adsorbent separation [26].

In this study, the effect of initial pH on adsorption capacity was studied by shaking 10 mg of $NH_2$-G with 25 ml solution (40 mg $L^{-1}$ MG) in different pH (from 3.0 to 11.0) for 150 min at 298 K. Fig. 3(a) shows the effect of solution pH for MG adsorption onto $NH_2$-G. The adsorption of MG increased with increasing pH, the highest adsorption (99.76%) was achieved at pH 11.0. The mechanisms of the adsorption process are likely to be the ionic interactions of the colored dye ions with the amino groups of the $NH_2$-G. As a basic dye, MG can generate cationic pigment ($MG^+$) in aqueous solution. At the same time, large numbers of $H^+$ present at low pH, which protonated the amino groups on the surface of $NH_2$-G [27].

$$\text{R-NH}_2 + \text{H}^+ \leftrightarrow \text{R-NH}_3^+ \text{ (amino protonate)}$$

That is the positive charge on the adsorbent inhibits the adsorption of dye in highly acidic solution [28]. In addition, at pH above 8, the present of large numbers of $OH^-$ ions makes $NH_2$-G more de-protonated with the decrease in acidity, which is helpful for the adsorption due to the electrostatic attraction between these two oppositely charged ions [29,30].

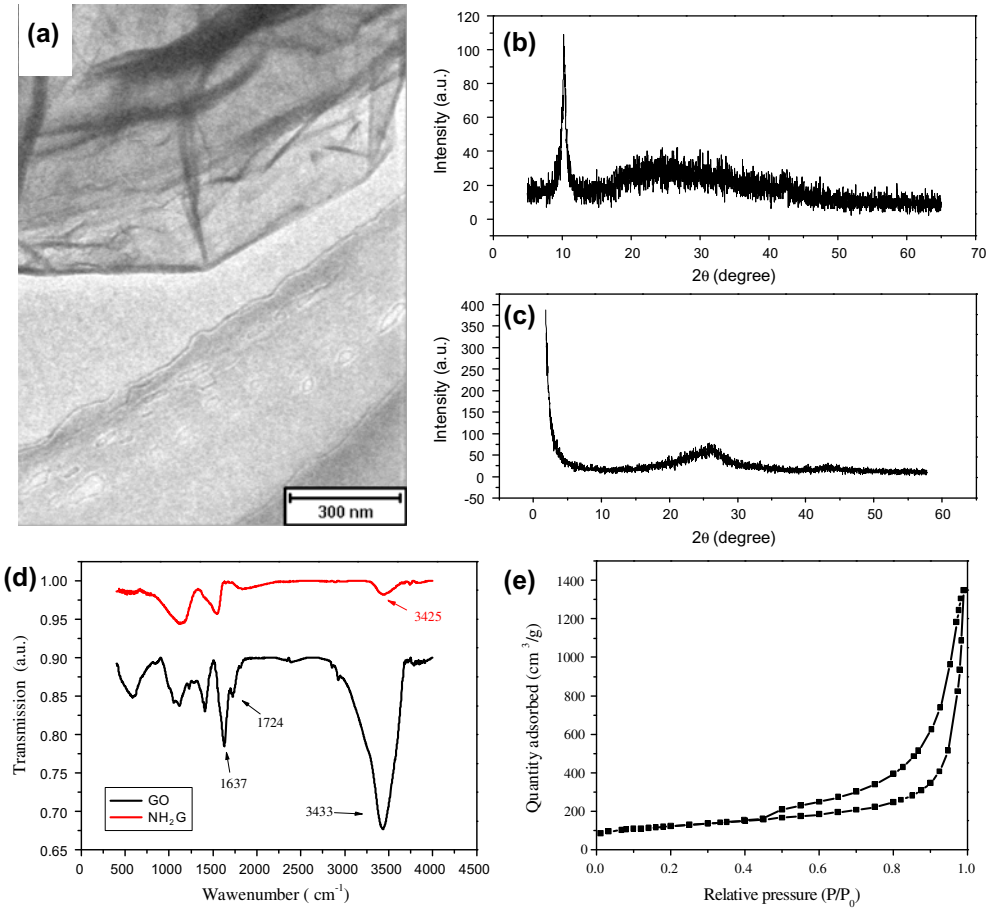


Fig. 2. TEM image of NH2-G (a), X-ray diffraction of GO (b), NH2-G (c), FTIR spectra analysis of NH2-G and GO (d), and BET analysis of NH2-G (e).

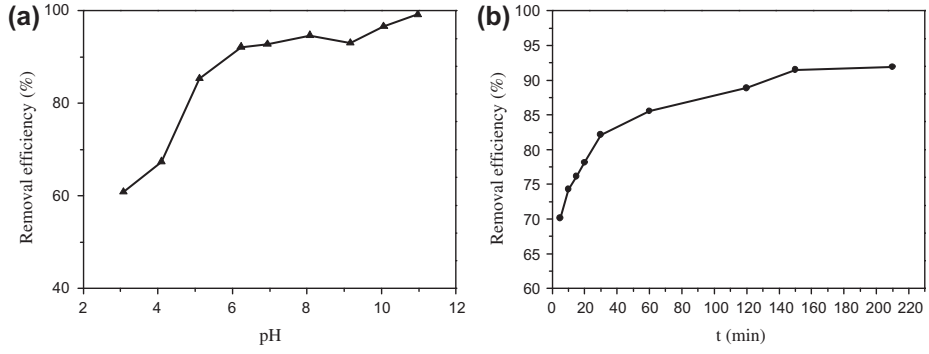


Fig. 3. Effect of initial pH on the adsorption of MG onto NH2-G (a) and contact time for adsorption of MG onto NH2-G (b).

$$\text{R-NH}_2 + \text{OH}^- \leftrightarrow \text{R-NH}^- + \text{H}_2\text{O} \text{ (amino de} - \text{protonate)}$$

$$\text{R-NH}^- + \text{MG}^+ \leftrightarrow \text{R-NH}\ldots\text{-MG} \text{ (ionic-pair formation)}$$

### 3.3. Mechanism discussion

Three possible mechanisms have been proposed to elucidate the adsorption of MG on $NH_2$-G, including

adsorption kinetic, adsorption isotherm and adsorption thermodynamic.

### 3.3.1. Adsorption kinetic

Adsorption is a time-dependent process, and therefore, the reaction speed and the relationship between the materials that participate in the reaction is highly important for design and evaluation of adsorbents in removing dyes from wastewater. The obtained adsorption date of MG on $NH_2$-G could analyze according to kinetic models expressed as follows:

pseudo-first-order kinetics:

$$q_t = q_e[1 - \exp(-k_1 t)] \tag{3}$$

pseudo-second-order kinetics:

$$q_t = \frac{k_2 t q_e^2}{1 + k_2 t q_e} \tag{4}$$

where $q_e$ (mg g$^{-1}$) is the amount of solute adsorbed at equilibrium, $q_t$ (mg g$^{-1}$) is the amount of solute adsorbent at time $t$, $k_1$ (min$^{-1}$) is the pseudo-first-order overall rate constant and $k_2$ (g mmol$^{-1}$ min$^{-1}$) is the rate constant for the pseudo-second-order equations.

The adsorption efficiency as a function of contact time was presented in Fig. 3(b). Fig. 3(b) shows that 150 min was need for $NH_2$-G to reach adsorption equilibrium, and the time curve could be divided into three portions, which could be indicated that intraparticle diffusion process might be one of the rate-limiting steps for MG removed by $NH_2$-G [31]. This phenomenon attribute to the pore size distribution of collectors and the size of dye [16]. The relative narrow pore size of $NH_2$-G makes dye to overcome high transport resistant from the micropores and migrating to contact with those active groups need longer time to reach equilibrium, which is consistent with the result of BET.

The adsorption kinetics data of dye were analyzed by pseudo-first-order kinetic model and pseudo-second-order kinetic model (Fig. 4). The modeled results of kinetics were listed in Table 1. The correlation coefficient of the second-order kinetic model for MG adsorb on $NH_2$-G are higher than 0.99, and the calculated $q_e$ value (92.59 mg g$^{-1}$) show good agreement with the experiment date (91.48 mg g$^{-1}$). The results indicate that the adsorption of MG on $NH_2$-G obey pseudo-second-order kinetics, suggesting a chemisorption process [32,33].

### 3.3.2. Adsorption isotherm

We selected four isotherm equations for the study of modeling these adsorption isotherm data: Temkin (Fig. 5(a)), Henry (Fig. 5(b)), Freundlich (Fig. 5(c)) and Langmuir (Fig. 5(d)) equations, expressed as follows:

Temkin model:

$$q_e = \frac{RT}{b_T} \ln c_e + \frac{RT}{b_T} \ln A_T \tag{5}$$

Henry model:

$$q_e = k c_e \tag{6}$$

Freundlich model:

$$q_e = K_F c_e^{1/n} \quad \ln q_e = \ln K_F + \frac{1}{n} \ln c_e \tag{7}$$

Langmuir model:

$$q_e = \frac{b q_m C_e}{1 + b C_e} \quad \frac{1}{q_e} = \frac{1}{b q_m} \cdot \frac{1}{c} + \frac{1}{q_m} \tag{8}$$

The adsorption capacity of $NH_2$-G to MG was measured individually at pH 8.0 with 10 mg of collector and varied dye concentration. The fitting results get from the isotherms were shown in Fig. 5, and the values of correlation coefficients obtained from the adsorbent were given in Table 2.

As seen in Table 2, it is found that the adsorption process of MG on $NH_2$-G can be better described by the Freundlich modal which assumes heterogeneous adsorption due to the diversity of adsorption sites. According to the $K_f$, it can be seen that the adsorption capacity increases with temperature. The value of $1/n$ was between 0 and 1, representing that the adsorption processes are favorable.

### 3.3.3. Adsorption thermodynamic

The study of temperature effect on MG adsorption onto collector was carried out at temperatures ranging from 298 to 318 K. In this contest, the systems were evaluated by calculating the values of variation of Gibbs free energies ($\Delta G$) obtained at different temperature tests. The enthalpy change ($\Delta H$) and entropy change ($\Delta S$) can also be determined by the following equations:

$$\Delta G = -RT \ln K_d \tag{9}$$

$$\ln K_d = \frac{\Delta S}{R} - \frac{\Delta H}{RT} \tag{10}$$

where $R$ (8.314 J mol$^{-1}$ K$^{-1}$) is the gas constant, $T$ (K) is the absolute temperature, and $K_d$ is the thermodynamic

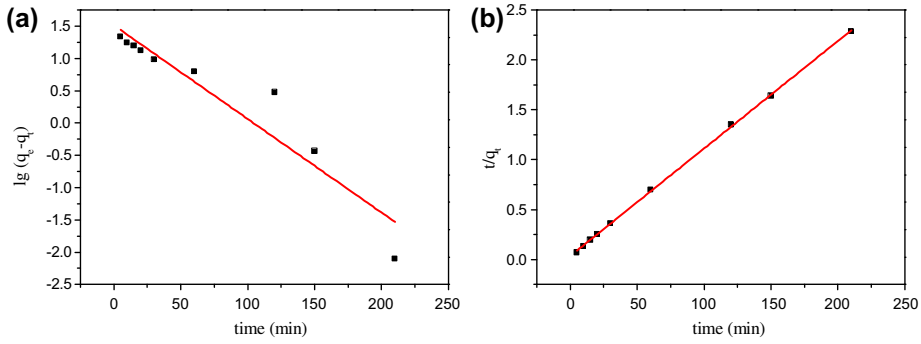


Fig. 4. Pseudo-first-order kinetics (a) and pseudo-second-order kinetics (b), for adsorption of MG onto NH2-G.

Table 1
Kinetic parameters for adsorption MG onto $NH_2$-G

| | Pseudo-first-order model | | | Pseudo-second-order model | | | |
|---|---|---|---|---|---|---|---|
| | $q_e$ (mg g$^{-1}$) | $k_1$ (min$^{-1}$) | $R^2$ | $q_e$ (mg g$^{-1}$) | $k_2$ (mg g$^{-1}$min$^{-1}$) | $R^2$ | $q_{e(exp)}$ (mg g$^{-1}$) |
| MG | 4.538 | 0.01450 | 0.8918 | 92.59 | $3.218 \times 10^{-3}$ | 0.9996 | 91.48 |

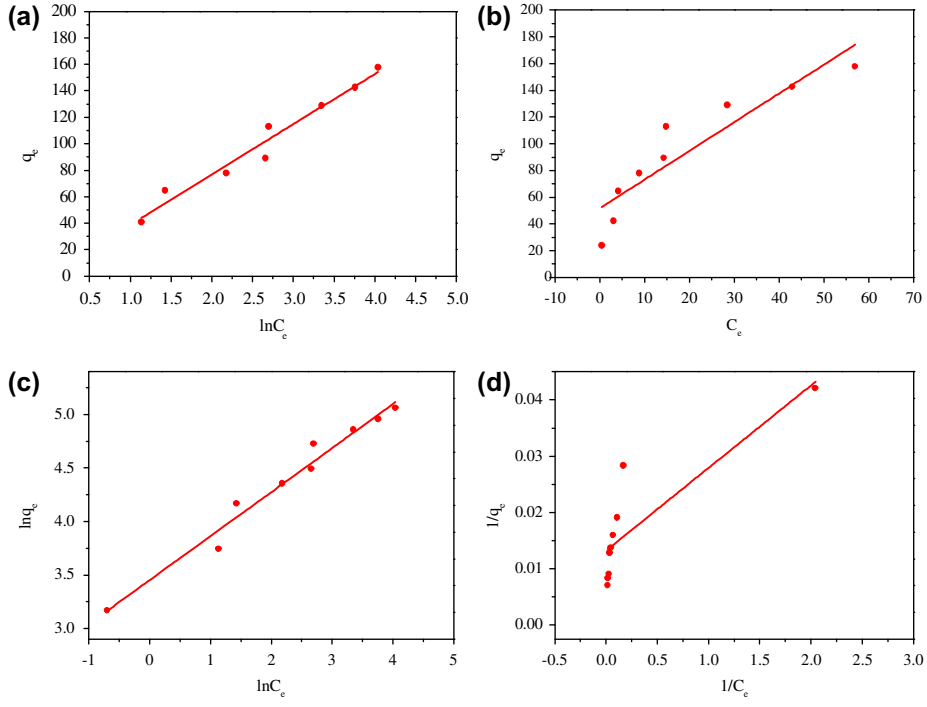


Fig. 5. Temkin (a), Henry (b), Freundlich (c), and Langmuir (d), adsorption isotherm fit of MG adsorption onto NH2-G.

equilibrium constant. The result of $\Delta G$, $\Delta H$, and $\Delta S$ are shown in Fig. 6. All the thermodynamic parameters are listed in Table 3.

With the temperature increased from 298 to 318 K, the values of $\Delta G$ decreased from −2.702 to −3.800 kJ mol$^{-1}$. The negative value of $\Delta G$ for MG shows that the adsorption process is spontaneous and endothermic reaction. The positive value of $\Delta H$ (15.64 kJ mol$^{-1}$) further demonstrated the endothermic process, and the value of $\Delta H$ is high enough to ensure strong interaction between the dye molecules and the adsorbent. An other important fact to be consider is

Table 2
Constants and correlation coefficients of adsorption isotherms for the adsorption

| Model | Parameter | $NH_2$-G |
|---|---|---|
| Temkin equation | $b_T$ | 67.33 |
| | $A_T$ | 1.018 |
| | $R^2$ | 0.9656 |
| Henry | $K_h$ | 2.149 |
| | $R^2$ | 0.8451 |
| Freundlich equation | $K_f$ | 31.54 |
| | $n$ | 2.429 |
| | $R^2$ | 0.9732 |
| Langmuir equation | $q_m$ (mg g$^{-1}$) | 104.2 |
| | $b$ (L mg$^{-1}$) | 0.8980 |
| | $R^2$ | 0.5679 |

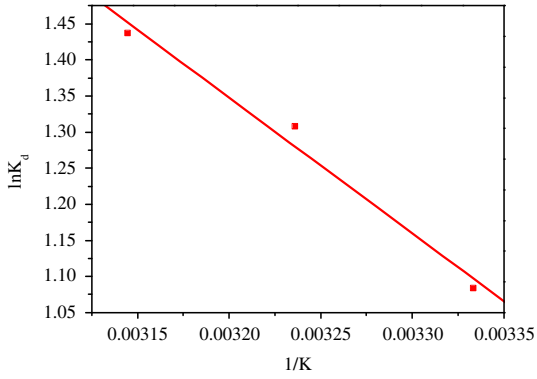


Fig. 6. Adsorption thermodynamics of MG adsorption onto NH2-G.

Table 3
Thermodynamic parameters of the adsorption of MG by $NH_2$-G

| Temperature ($K$) | $\Delta G$ (kJ mol$^{-1}$) | $\Delta H$ (kJ mol$^{-1}$) | $\Delta S$ (J mol$^{-1}$ K$^{-1}$) |
|---|---|---|---|
| 298 | −2.702 | 15.64 | 61.24 |
| 308 | −3.535 | | |
| 318 | −3.800 | | |

that the adsorption capacity of $NH_2$-G increase with the temperature rises indicating an endothermic process, which in accordance with the principles of chemical adsorption. Taking into considerate the result of kinetic, isotherm and thermodynamic, the adsorption of MG by $NH_2$-G is a chemical process.

## 4. Conclusion

In the study, batch equilibrium adsorption of MG onto $NH_2$-G was carried out under various conditions, that is, the solution pH, the contact time, the initial concentration and the temperature. The results indicate that the $NH_2$-G could be considered as a good alternative with large surface area and functional group for extracting the tested acid dye from aqueous media. The kinetic evaluation of the adsorption showed that the adsorption agree well to pseudo-second-order kinetic model. The adsorption isotherms of MG onto $NH_2$-G could be described well by the Freundlich isotherm model. Furthermore, the thermodynamic studies illustrate that the adsorption process of MG onto $NH_2$-G was endothermic and spontaneous in nature. The adsorption capacity of $NH_2$-G is over 90 mg g$^{-1}$ at optimized condition. The results show that the adsorption capacity of basic dye by $NH_2$-G is high.

## Acknowledgments

This study was supported by the Natural Science Foundation of China (No. 21075052, 21175057, 21375047, 21377046), the Natural Science Foundation of Shandong Province (No. ZR2010EM063) and QW thanks the Special Foundation for Taishan Scholar Professorship of Shandong Province and UJN.

## References

[1] F. Bangash, A. Manaf, Thermodynamics of basic dyes (Methylene blue and Basic blue 3) adsorption on active charcoal prepared from the wood of *Ailanthus altisima*, J. Chem. Soc. Pak. 28 (2011) 20–26.
[2] Q.C. Ge, P. Wang, C.F. Wan, T.S. Chung, Polyelectrolyte-promoted forward osmosis-membrane distillatio(FO-MD) hybrid process for dye wastewater treatment, Environ. Sci. Technol. 46 (2012) 6236–6243.
[3] K. Shakir, A.F. Elkafrawy, H.F. Ghoneimy, S.G.E. Beheir, M. Refaat, Removal of rhodamine B (a basic dye) and thoron (an acidic dye) from dilute aqueous solutions and wastewater simulants by ion flotation, Water Res. 44 (2010) 1449–1461.
[4] Y. Kisir, A.Z. Aroguz, Adsorption characteristics of the hazardous dye brilliant green on saklikent mud, Chem. Eng. J. 172 (2011) 199–206.
[5] P. Waranusantigul, P. Pokethitiyook, M. Kruatrachue, E.S. Upatham, Kinetics of basic dye (methylene blue) biosorption by giant duckweed (Spirodela polrrhiza), Environ. Pollut. 125 (2003) 385–392.
[6] J.L. Gong, B. Wang, G.M. Zeng, C.P. Yang, C.G. Niu, W.J. Zhou, Y. Liang, Removal of cationic dyes from aqueous solution using magnetic multi-wall carbon nanotube nanocomposite as sorbent, J. Hazard. Mater. 164 (2009) 1517–1522.
[7] M. Kornaros, G. Lyberatos, Biological treatment of wastewaters from a dye manufacturing company using a trickling filter, J. Hazard. Mater. 136 (2006) 95–102.
[8] E. Guibal, J. Roussy, Coagulation and flocculation of dye-containing solutions using a biopolymer (Chitosan), React. Funct. Polym. 67 (2007) 33–42.
[9] W. Zhao, Z. Wu, D. Wang, Ozone direct oxidation kinetics of cationic red X-GRL in aqueous solution, J. Hazard. Mater. 137 (2006) 1859–1865.

[10] K. Dutta, S. Mukhopadhyaya, S. Bhattacharjee, B. Chaudhuri, Chemical oxidation of methylene blue using a Fenton-like reaction, J. Hazard. Mater. 84 (2001) 57–71.
[11] G. Capar, U. Yetis, L. Yilmaz, Membrane based strategies for the pre-treatment of acid dye bath wastewaters, J. Hazard. Mater. 135 (2006) 423–430.
[12] C.H. Liu, J.S. Wu, H.C. Chiu, S.Y. Suen, K.H. Chu, Removal of anionic reactive dyes from water using anion exchange membranes as adsorbers, Water Res. 41 (2007) 1491–1500.
[13] M. Muruganandham, M. Swaminathan, TiO2–UV photocatalytic oxidation of reactive yellow 14: Effect of operational parameters, J. Hazard. Mater. 135 (2006) 78–86.
[14] R. De Lisi, G. Lazzara, S. Milioto, N. Muratore, Adsorption of a dye on clay and sand. Use of cyclodextrins as solubility-enhancement agents, Chemosphere 69 (2007) 1703–1712.
[15] Philip Bradder, Sie King Ling, Shaobin Wang, Shaomin Liu, Dye adsorption on layered graphite oxide, J. Chem. Eng. Data 56 (2011) 138–141.
[16] L.F. Lai, L.W. Chen, D. Zhan, L. Sun, J.P. Liu, S.H. Lim, C.K. Poh, Z.X. Shen, J.Y. Lin, One-step synthesis of $NH_2$-graphene from *in situ* graphene-oxide reduction and its improved electrochemical properties, Carbon 49 (2011) 3250–3257.
[17] H.L. Guo, X.F. Wang, Q.Y. Qian, F.B. Wang, X.H. Xai, A green approach to the synthesis of grapheme nanosheets, ACS Nana. 3 (2009) 2653–2659.
[18] W. Lv, D.M. Tang, Y.B. He, C.H. You, Z.Q. Shi, X. Chen, C. M. Chen, P.X. Hou, C. Liu, Q.H. Yang, Low-temperature exfoliated graphemes: Vacuum-promoted exfoliation and electrochemical energy storage, ACS Nano. 3 (2009) 3730–3735.
[19] G.X. Zhao, J.X. Li, X.G. Wang, Kinetic and thermodynamic study of 1-naphthol adsorption from aqueous solution to sulfonated graphene nanosheets, Chem. Eng. J. 173 (2011) 185–190.
[20] G.X. Zhao, L. Jiang, Y.D. He, J.X. Li, H.L. Dong, X.K. Wang, Sulfonated graphene for persistent aromatic pollutant management, Adv. Mater. 23 (2011) 3959–3963.
[21] L. Sun, H.W. Yu, B. Fugetsu, Graphene oxide adsorption enhanced by *in situ* reduction with sodium hydrosulfite to remove acridine orange from aqueous solution, J. Hazard. Mater. 203 (2012) 101–110.
[22] V. Chandra, J. Park, Y. Chun, J.W. Lee, I.C. Hwang, K.S. Kim, Waterdispersible magnetite-reduced graphene oxide composites for arsenic removal, ACS Nano. 4 (2010) 3979–3986.
[23] F. Barroso-Bujans, S. Cerveny, R. Verdejo, J.J. del Val, J.M. Alberdi, A. Alegria, J. Colmenero, Permanent adsorption of organic solvents in graphite oxide and its effect on the thermal exfoliation, Carbon 48 (2010) 1079–1087.
[24] D.C. Marcano, D.V. Kosynkin, J.M. Berlin, A. Sinitskii, Z.G. Sun, A. Slesarev, L.B. Alemany, W. Lu, J.M. Tour, Improved synthesis of grapheme oxide, J. Am. Chem. Soc. 4 (2010) 4806–4814.
[25] K.J. Huang, D.J. Niu, J.Y. Sun, J.J. Zhu, An electrochemical amperometric immunobiosensor for label-free detection of α–fetoprotein based on amine-functionalized grapheme and gold nanoparticles modified carbon ionic liquid electrode, J. Electroanal. Chem. 656 (2011) 72–77.
[26] P.P. Selvam, S. Preethi, P. Basakaralingam, N. Thinakaran, A. Sivasamy, S. Sivanesan, Removal of rhodamine B from aqueous solution by adsorption onto sodium montmorillonite, J. Hazard. Mater. 155 (2008) 39–44.
[27] L. Sun, H. Yu, B. Fugetsu, Graphene oxide adsorption enhanced by *in situ* reduction with sodium hydrosulfite to remove acridine orange from aqueous solution, J. Hazard. Mater. 203 (2012) 101–110.
[28] M. Srinivasan, C. Ferrarris, T. White, Cadmium and lead ion capture with three dimensionally ordered macroporous hydroxyapatite, Environ. Sci. Technol. 40 (2006) 7054–7049.
[29] E. Sudova, J. Machova, Z. Svobodova, T. Vesely, Negative effects of malachite green and possibilities of its replacement in the treatment of fish eggs and fish: A review, Vet. Med. 52 (2007) 527–539.
[30] L.M. Zhou, J.Y. Jin, Z.R. Liu, X.Z. Liang, C. Shang, Adsorption of acid dyes from aqueous solutions by the ethylenediamine-modified magnetic chitosan nanoparticles, J. Hazard. Mater. 185 (2011) 1045–1052.
[31] S.D. Pan, Y. Zhang, H.Y. Shen, M.Q. Hu, An intensive study on the magnetic effect of mercapto-functionalized nanomagnetic $Fe_3O_4$ polymers and their adsorption mechanism for the removal of Hg(Ⅱ) for aqueous solution, Chem. Eng. J. 210 (2012) 564–574.
[32] G. Crini, H.N. Peindy, F. Gimbert, C. Robert, Removal of C.I. basic green 4 (malachite green) from aqueous solutions by adsorption using cyclodextrinbased adsorbent: Kinetic and equilibrium studies, Sep. Purif. Technol. 53 (2007) 97–110.
[33] Y.S. Ho, Review of second-order models for adsorption systems, J. Hazard. Mater. 136 (2006) 681–689.